PNAS
www.pnas.org

Supplementary Information for

Bacterial endosymbionts protect beneficial soil fungus from nematode attack

Hannah Büttner,[†,1] Sarah P. Niehs,[†,1] Koen Vandelannoote,[2] Zoltán Cseresnyés,[3] Benjamin Dose,[1] Ingrid Richter,[1] Ruman Gerst,[3,4] Marc Thilo Figge,[3,5] Sacha J. Pidot,[*,2] Christian Hertweck[*,1,4]

Corresponding authors: Christian Hertweck, Sacha J. Pidot
* To whom correspondence may be addressed. Email: christian.hertweck@leibniz-hki.de; sacha.pidot@unimelb.edu.au

This PDF file includes:

Other supplementary materials for this manuscript include the following:

Experimental Procedures

Bacterial and fungal strains

Strains of this study are listed in Table S 1. All media used in this study are listed in Table S 2. Sterilization of the media took place at 120 °C for 20 min.

Burkholderia sp. strain B8 (HKI-0404; syn. *Mycetohabitans*) (1) was isolated from *Rhizopus microsporus* Tieghem var. *microsporus* CBS 308.87 by subsequent procedure: The fungus was inoculated into MGY+M9 medium and grown at 30 °C and 110 rpm until increasing turbidity of the medium was observed by eye. The culture was centrifuged (12,000 × *g*, 10 min, 25 °C). A small volume was separated from the upper surface of the culture and spread on NAG agar. After growth at 30 °C for 3–4 days, bacterial colonies were inoculated into MGY+M9 medium and slowly upscaled.

Fungal spores were stored in 50 % glycerol at –20 °C for long-term storage. For short-term storage they were grown on PDA and kept at 4 °C or room temperature.

Table S 1. Strains used in this study.

Strain	No.	Original site of isolation
Burkholderia sp.	HKI0404, strain B8	CBS 308.87 in this study
Rhizopus microsporus Tieghem var. *microsporus*	CBS 308.87 (NRRL 28628)	Human necrotic tissue after a spider bite, Australia
Candidatus Mycoavidus necroximicus	-	*Mortierella verticillata* NRRL 6337
Mortierella verticillata	NRRL 6337 (CBS 131.66)	Sandy forest soil, United Kingdom
Mortierella verticillata	NRRL 6369 (CBS 100561)	Soil of Great Bear Lake, Canada
Mortierella verticillata	SF9852 (CBS 346.66)	Tundra soil, Alaska
Mortierella verticillata	SF9853 (CBS 220.58)	Soil under *Betula* sp., France
Mortierella verticillata	SF9854 (CBS 225.35)	Former West Germany
Mortierella verticillata	SF9856 (CBS 315.52)	Forest soil, former West Germany
Escherichia coli	OP50	-
Caenorhabditis elegans	Wild-type N2 (var. Bristol)	-
Aphelenchus avenae	Bastian, 1865	-

Table S 2. Media used in this study.

Media	Composition (L^{-1})
MGY+M9 medium	10 g Glycerol, 1.25 g yeast extract (autolyzed yeast cells, BD, Bacto), 960 mL water, sterilization, add: 20 mL M9 salt A, 20 mL M9 salt B
MM9 medium	2 g Amino acid mix, 10 g glycerol, 900 mL water, sterilization, add: appropriate antibiotics, 20 mL M9 salt A, 20 mL M9 salt B, 16.8 mL L-leucine solution (100 mM), 5 mL L-histidine solution (60 mM), each 10 mL of L-lysine (100 mM), L-tryptophan (40 mM), L-methionine solution (40 mM), 2 mL vitamin solution, 1 mL trace element solution
PDB/PDA	Potato dextrose broth or agar (BD, Bacto), sterilization
NAG agar	Standard nutrient agar I (Merck), 10 g glycerol, sterilization
Modified medium 2	3 % Glycerol, 1 % glucose, 0.5 % peptone, 0.2 % NaCl, pH 6.0, sterilization
LB	Lysogeny broth (BD, Bacto), sterilization
TSB	Tryptone soy broth (BD, Bacto), sterilization
CYE	Charcoal yeast extract medium; 10 g yeast extract (autolyzed yeast cells, BD, Bacto), 10 g ACES, 1 g potassium oxoglutamate, 2 g active charcoal, pH 6.9, sterilization, add: 0.25 g Fe-pyrophosphate (sterile filtered)
K-medium	3.1 g NaCl, 2.4 g KCl, sterilization
NGM	3 g NaCl, 2.5 g peptone (BD, Bacto), 17 g agar, sterilization, add (sterile): 5 mg cholesterol, 0.11 g $CaCl_2$, 0.25 g $MgSO_4$, 2.7 g KH_2PO_4, 0.89 g K_2HPO_4
M9 salts A	350 g K_2HPO_4, 100 g KH_2PO_4, sterilization
M9 salts B	29.4 g Sodium citrate, 50 g $(NH_4)_2SO_4$, 5 g $MgSO_4$, sterilization
Amino acid mix	L-Amino acids in equal amounts: alanine, asparagine, cysteine, glutamate, isoleucine, serine, arginine, aspartate, glutamine, glycine, proline, threonine, valine
Vitamin solution	10 mg Folic acid, 6 mg biotin, 200 mg *p*-aminobenzoic acid, 1 g thiamine-HCl, 1.2 g pantothenic acid, 1 g riboflavin, 2.3 g nicotinic acid, 12 g pyridoxine HCl, 100 mg vitamin B_{12}
Trace element solution	40 mg $ZnCl_2$, 200 mg $FeCl_3 \times 6\ H_2O$, 10 mg $CuCl_2 \times 2\ H_2O$, 10 mg $MnCl_2 \times 4\ H_2O$, 10 mg $Na_2B_4O_7 \times 10\ H_2O$, 10 mg $(NH_4)_6Mo_7O_{24} \times 4\ H_2O$

Identification of endosymbionts in *Mortierella verticillata*

Amplification of bacterial 16S rDNA and phylogenetic analysis. Fungal strains were cultivated in MM9 medium at 26 °C and orbital shaking at 110 rpm. The genomic DNA was isolated either from the turbid supernatant or the disrupted fungus itself with the MasterPure DNA Purification Kit (Epicentre). 16S rDNA was amplified using gDNA, the primers 8F (AGA GTT TGA TCC TGG CTC AG) and 1492R (CGG TTA CCT TGT TAC GAC TT) with Phusion High-Fidelity PCR Master Mix with HF Buffer (NEB). PCR program: 30 cycles of 95 °C for 15 s, 65 °C for 15 s, 72 °C for 1 min 40 s.

The 16S rDNA sequences of the *Mortierella* endosymbionts
were uploaded to the NCBI database:
BRE_MvertCBS_346.66 MZ330684;
BRE_MvertCBS_220.58 MZ330685;
BRE_MvertCBS_225.35 MZ330686;
BRE_MvertCBS_315.52 MZ330687;
BRE_MvertCBS_100561 MZ330688.

Phylogenetic analysis of 16S rDNA of *Mortierella* endosymbionts (and further representatives of the Burkholderiaceae family) were performed as follows: The sequence alignment was performed using Clustal Omega with default settings (2). Maximum likelihood phylogeny was constructed using IQ-tree 2. Ultrafast bootstrapping (1,000 iterations) analysis was performed (3). Bootstrap values >80 % are shown at nodes. *Wolbachia pipientis* (16S rDNA gene sequence accession number: AY833061.1) was used as outgroup. Sequences where retrieved from the NCBI database, grouping of sequences to clades was performed in accordance to (4) (Figure S 3).

Preparation of aposymbiotic fungal strains. Fungal strains were continuously cultivated at 24 °C on PDA plates (Bacto, BD) containing 40 µg mL^{-1} ciprofloxacin or 50 µg mL^{-1} kanamycin for 4 months. After phenotypical changes were observed by eye, the *M. verticillata* NRRL 6337 fungal cultures were extracted with 1:1 volume of ethyl acetate and checked for production of **3** and **4**. Amplification of bacterial 16S rDNA from cured fungi did not lead to any amplicon (Figure S 2). Final examination of the cured fungal strains occurred by fluorescent staining.

Fluorescent staining. Fungal strains (wild type and aposymbiotic strains) were visualized by a Zeiss LSM 710 confocal laser-scanning microscope. First, fungal hyphae were stained with Calcofluor White Stain (Sigma) and SYTO 9 Green (Invitrogen) for 5 min, then washed in 0.85 % NaCl solution, and checked for endosymbionts. Wavelengths were adjusted as specified by the manufacturer (Figures S 1–S 2).

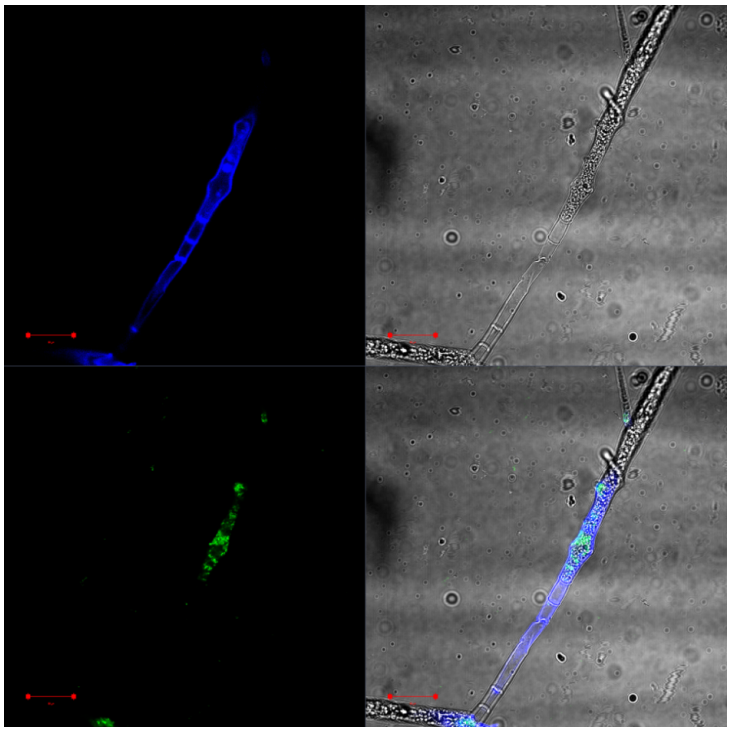

Figure S 1. Fluorescence microscopy image of *M. verticillata* NRRL 6337. Channel 1 Calcofluor White staining (to stain the fungal cell wall, blue; top left), channel 2 bright field (top right), channel 3 SYTO 9 Green (to stain nucleic acids and visualize bacteria, green; bottom left), channel 4 overlay (bottom right). Scale matches 20 µm.

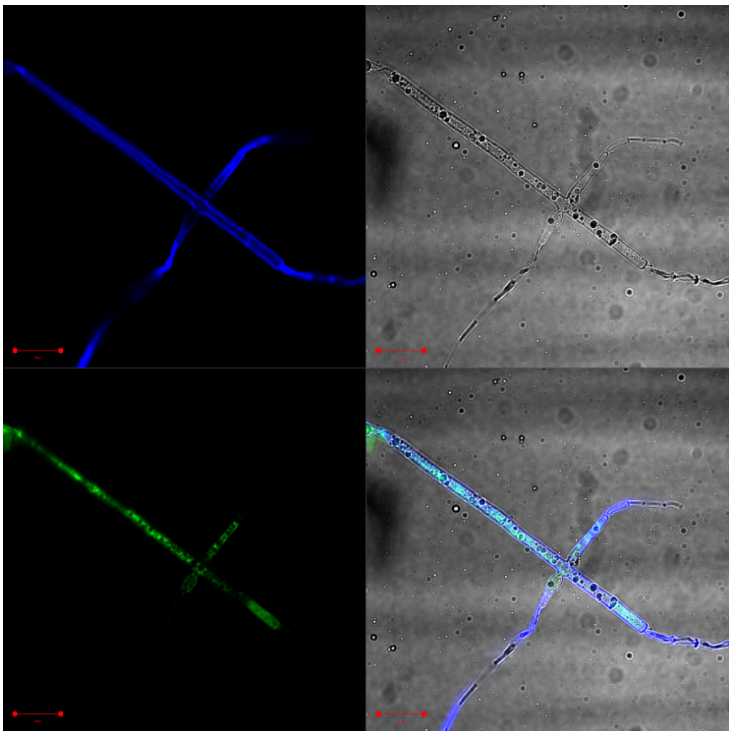

Figure S 2. Fluorescence microscopy image of cured (aposymbiotic) *M. verticillata* NRRL 6337. Channel 1 Calcofluor White staining (to stain the fungal cell wall, blue; top left), channel 2 bright

field (top right), channel 3 SYTO 9 Green (to stain nucleic acids and visualize bacteria, green; bottom left) (overexposure), channel 4 overlay (bottom right). Scale matches 20 µm.

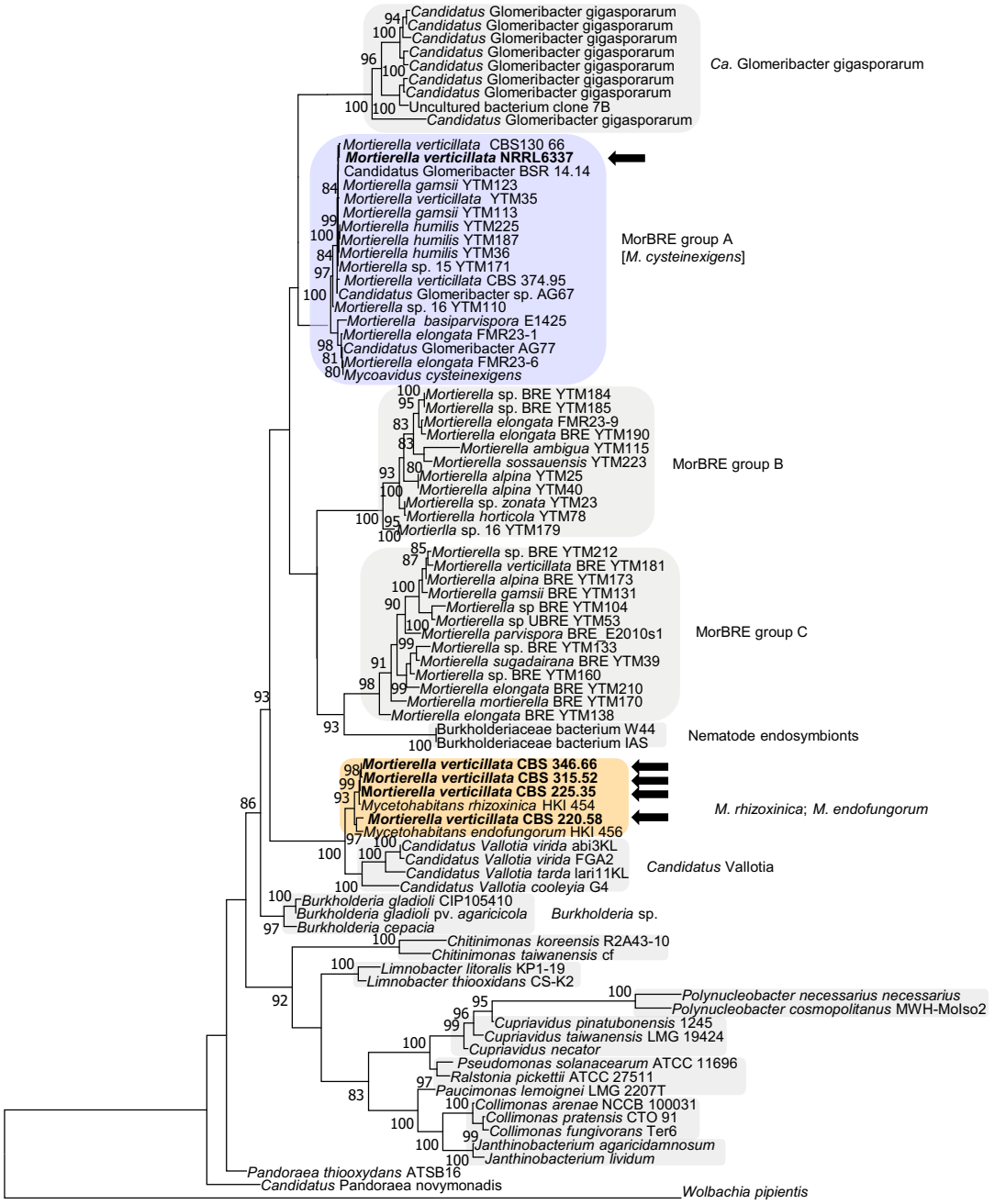

Figure S 3 Phylogenetic analysis of amplified 16S rDNA from *Mortierella* symbionts. Strains of this study are marked with an arrow. Additional bacterial sequences labelled "*Mortierella*" were extracted from a previous publication (4). Abbreviation: BRE *Mortierella*, *Burkholderia*-related endosymbiont of *Mortierella* spp.

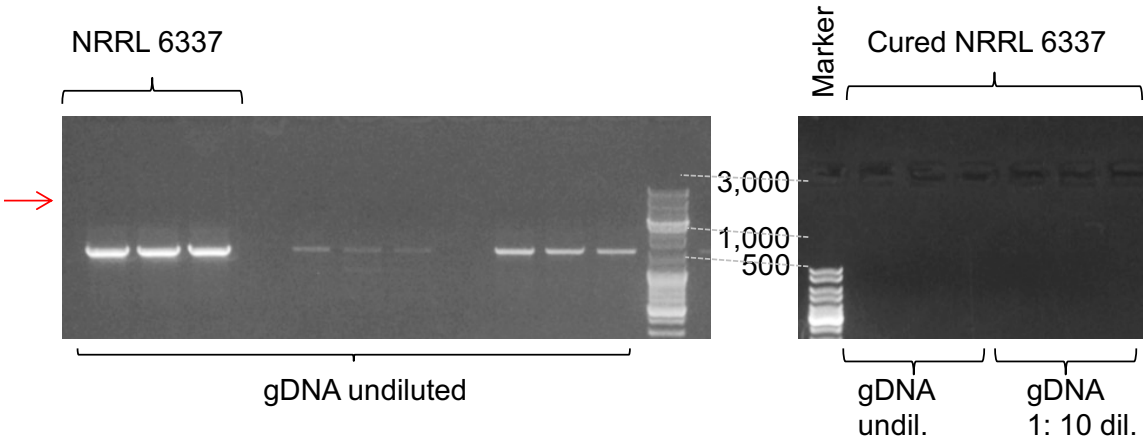

Figure S 4 Amplification of bacterial 16S rDNA from symbiotic and cured *M. verticillata* NRRL 6337 strains using the primers 8F (AGA GTT TGA TCC TGG CTC AG) and 1492R (CGG TTA CCT TGT TAC GAC TT**)**. Marker in Da. Undil, not diluted. Marker sizes in Da.

Endosymbiont isolation attempts (for *M. verticillata* spp.). In short, isolation attempts include bacteria derived from turbid supernatant of fungal cultures or from disrupted hyphae (homogenizer or bead mill). The bacterial mixture was filtered through a 40 µm sieve (Corning Cell Strainer) and a 5 µm filter (Cameo, Roth) before inoculation. Tested media included: MGY+M9, MM9, PDB, NAG, LB, TSB, CYE medium (5), as well as CYE medium containing autoclaved or sterile filtered *M. verticillata* cultures grown in PDB. The same media were also tested with additional L-cysteine, amino acid mix solution (Table S 2) and 3 % glycerol. Every assay was performed with liquid medium and/or on an agar plate. If fungal growth occurred on plates, these parts were cut out with a sterile scalpel. For liquid media also the addition of amphotericin in concentrations of 1 µM, 5 µM or 10 µM was tested to inhibit fungal growth. Cultures were incubated at 20 °C, 26 °C, 30 °C and 37 °C for up to 30 days. Additionally, the infection of a cured fungal strain with bacterial filtrate did not result in living endosymbionts.

Genome assembly for *Candidatus* Mycoavidus necroximicus

M. verticillata NRRL 6337 was grown in 3 L MM9 medium (Table S 2) with orbital shaking at 160 rpm and 26 °C. Mild physical sheering through shaking culture in baffled flasks led to increasing turbidity of the culture supernatant over time. Microscopic analysis revealed a high number of bacteria in comparison to mycelia in the turbid medium. The cultures were controlled for turbidity by eye every day. If the supernatant turned significantly turbid, the culture was twice filtered through a membrane (pore diameter 40 µm; Corning cell strainer) and centrifuged (12,000 × *g*, 25 °C, 10 min) until a stabile pellet occurred. The genomic DNA was extracted according to manufacturer's recommendations with the MasterPure DNA Purification Kit (Epicentre).
The extracted gDNA from *M. verticillata* was prepared for sequencing on both the Oxford Nanopore MinION and Illumina NextSeq platforms. For long-read sequencing on the MinION platform, DNA quality was evaluated by pulsed-field gel electrophoresis and prepared for sequencing according to the protocol of the Ligation Sequencing kit (Oxford Nanopore). DNA was loaded onto a single MinION flow cell and data was collected over a 72 hour period. DNA was prepared for sequencing on the Illumina NextSeq platform using the Nextera XT DNA preparation kit (Illumina) with × 150 bp paired end chemistry and with a targeted sequencing depth of >50 ×. Combined MINion and Illumina sequencing data were assembled using the Unicycler hybrid assembler (6, 7), following which a single contig 2.2 Mb containing a 98.82 % match to the *Mycoavidus cysteinexigens* 16S rDNA gene was extracted and evaluated for secondary metabolite loci using antiSMASH version 5 (8).

Identification and annotation of secondary metabolite gene cluster

Candidatus Mycoavidus necroximicus differed from other so far characterized *Mycoavidus* species. In contrast, we identified many similarities in the natural product arsenal between the *Mortierella* symbiont *Candidatus* Mycoavidus necroximicus and symbionts of *R. microsporus* along with their overall high potential for secondary metabolism. In addition to the necroximes (**3** and **4**), also the lasso peptide mycetohabin-15 (**8**) (35), originally reported from the fungal endosymbiont *Mycetohabitans* (previously *Paraburkholderia*) *rhizoxinica*, was detected from cultures of *Candidatus* Mycoavidus necroximicus (Figure S 5). Furthermore, through intensified bioinformatics analyses all genes necessary for F420 biosynthesis were identified, an important redox co-factor (9-11) that has been described in endofungal *Burkholderia* sp. and other bacteria before. For the detection of secondary metabolites antiSMASH (8) and PKS/NRPS analysis (12) were used for annotation of the biosynthetic gene cluster and the necroxime cluster (Figure S 6). Available genome assemblies of *Mycoavidus cysteinexigens* AG77 (13), B2-EB (14) and B1-EB^T (15) were processed in the same way. In addition, precursor sequences coding for lasso peptide assembly were identified manually (putative core peptides are highlighted in bold; putative cyclization sites in red):

a) *Candidatus* Mycoavidus necroximicus

MTKSKAINTQEIQLDDDALMEFCASESTM	**GAVGEKNEAGFGKYDDDAV**
MIKNQELNSQAIQLDDEALTQFSASEATM	**GGSGQYREAGVGRFL*** (Mycetohabin-15)
MTDSKKTTTQDTQLKDEALTEFCASESTM	**GGSGQYREAGVGRFL*** (Mycetohabin-15)

b) *M. cysteinexigens* AG77

MIKNQELNQDIQLDDEALTQFCASEATM	**GGSGQYKEAGVGRFL***
MIKNQELNQDIQLDDEVLTQFCASEATM	**GGSGKYKEAGVGRFL***
MTNSKEIKIQETQLQDETLSEFCASKATM	**GGSGQYREAGVGRFL** (Mycetohabin-15)
MTKSKELSQDIQLEETLMEFCASEATM	**GAVGEKNEAGFGKY**

c) *M. cysteinexigens* B1-EB^T

MIKNQELNQDIQLDDEVLTQICASEATM	**GGSGQYREAGVGRFL*** (Mycetohabin-15)
MIKNQELNQDIQLDDEVLTQFCASEATM	**GGSGKYKEAGVGRFL**
MTKSKELSQDIQLEETLMEFCASEATM	**GAVGEKNEAGFGKY**
MTNSKENKIQEIQLQDETLSEFCASEATM	**GGSGQYREAGVGRFL*** (Mycetohabin-15)

d) *M. cysteinexigens* B2-EB^T

MTNSKETKTQETQLQDETLSEFCASEATM	**GGSGQYREAGVGRFL** (Mycetohabin-15)

* 1–2 copies of the core peptide with different leader peptides detected in the genome (only assigned as one lassopeptide)

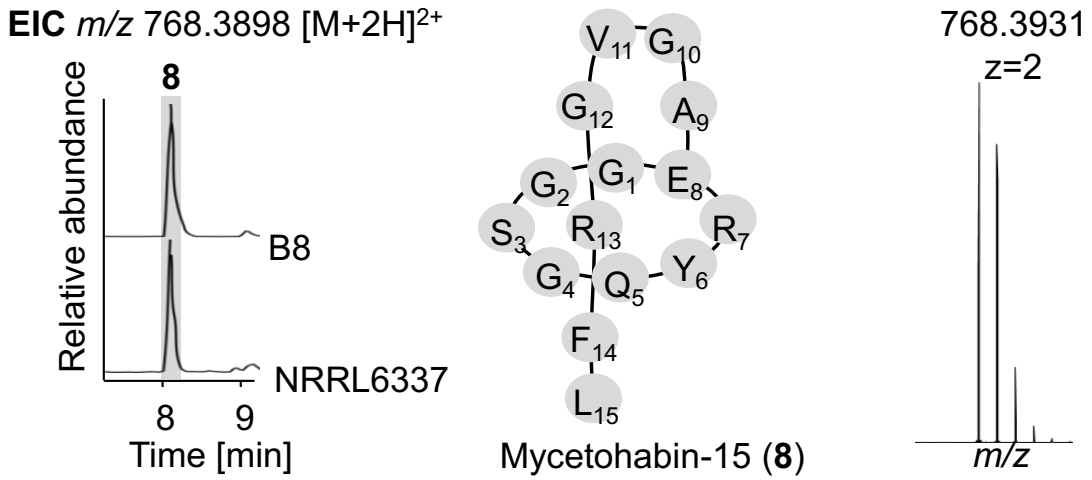

Figure S 5. Mycetohabin-15. Extracted ion chromatograms of mycetohabin-15 (**8**) (*m/z* 768.3930 [*M*+2H]$^{2+}$) observed in extracts of *Candidatus* Mycoavidus necroximicus (NRRL 6337) and *Burkholderia* sp. strain B8. Structure of the lasso peptide **8** and isotopic pattern.

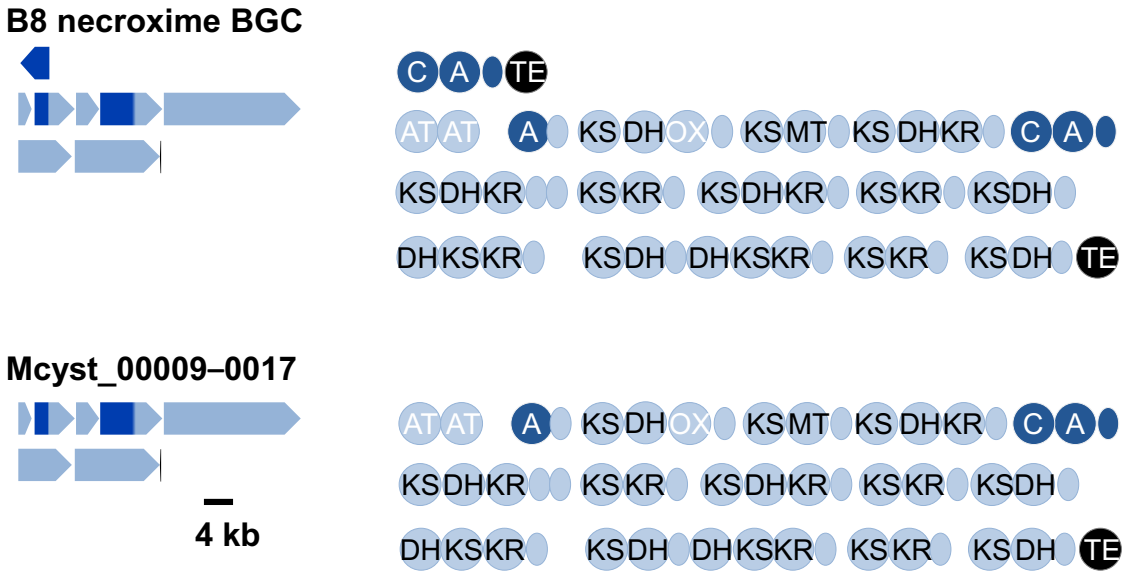

Figure S 6. Architectures of necroxime biosynthetic assembly lines in *Burkholderia* sp. strain B8 (top) and *Candidatus* Mycoavidus necroximicus (below).

Table S 3. Proteins encoded in the necroxime assembly line of *Candidatus* Mycoavidus necroximicus and putative up- and downstream proteins. Id./Sim. – Identity/Similarity.

Locus Mcyst_ 00	[bp]	Putative protein	SwissProt/ PDB entry	Acces-sion #	Organism	Id./ Sim.
024	1,191	Sodium/hydrogen exchanger	UPF0391 membrane protein XCV1406	Q3BVS6.1	*Xanthomonas campestris* pv. *vesicatoria* str. 85-10	35%/ 62%
023	1,116	Putative glutamate-cysteine ligase 2	Gamma-glutamyl-cysteine synthetase 2	B2T7N6.1	*Paraburk-holderia phytofirmans* PsJN	73%/ 86%
022	447	Hypothetical protein	Histone-lysine N-methyltrans-ferase 2A	Q03164.5	*Homo sapiens*	40%/ 55%
021	603	Hypothetical protein	Uncharacterized protein y4rO	P55648.1	*Sinorhizobium fredii* NGR234	33%/ 58%
020	876	IS982 family tranposase	Putative transposase	Q08082.2	*Brucella ovis* ATCC 25840	28%/ 44%
019	219	Hypothetical protein	-	-	-	-
018	190	Hypothetical protein	-	-	-	-
017	1,899	Malonyl CoA-acyl carrier protein transacylase	AT	A7Z4X8.1	*Bacillus velezensis* FZB42	48%/ 66%
016	5,541	PKS synthase/ NRPS synthetase	PKS	P40806.3	*Bacillus subtilis* subsp. *subtilis* str. 168	36%/ 51%
015	3,177	Polyketide synthase	PKS	P40806.3	*Bacillus subtilis* subsp. *subtilis* str. 168	33%/ 52%
014	8,541	PKS/NRPS	Polyketide synthase PksN	O31782.3	*Bacillus subtilis* subsp. *subtilis* str. 168	30%/ 47%
013	18,807	Polyketide synthase	PKS	P40806.3	*Bacillus subtilis* subsp. *subtilis* str. 168	31%/ 49%

Table S 3 continued. Proteins encoded in the necroxime assembly line of *Candidatus* Mycoavidus necroximicus and putative up- and downstream proteins. Id./Sim. – Identity/Similarity.

Locus Mcyst_ 00	[bp]	Putative protein	SwissProt/ PDB entry	Acces-sion #	Organism	Id./ Sim.
012	7,329	Polyketide synthase	PKS	P40806.3	*Bacillus subtilis* subsp. *subtilis* str. 168	43%/ 57%
011	11,652	Polyketide synthase	Polyketide synthase PksN	O31782.3	*Bacillus subtilis* subsp. *subtilis* str. 168	47%/ 63%
010	183	Hypothetical protein	Rho guanine nucleotide exchange factor 11	Q9ES67. 1	*Rattus norvegicus*	38%/ 47%
009	1,416	Epi-isozizaene 5-monooxygenase	Probable cytochrome P450 311a1	Q9VYQ7. 1	*Drosophila melanogaster*	28%/ 43%
008	237	Hypothetical protein	Glutamyl-tRNA(Gln) amidotrans-ferase subunit B-1	C1MIE8.1	*Micromonas pusilla* CCMP1545	32%/ 44%
007	1,665	Lanthionine synthetase C family protein	-	-	-	-
006	132	Hypothetical protein	-	-	-	-
005	1,038	Hypothetical protein	3-keto-5-aminohex-anoate cleavage enzyme	B0VHH0. 1	*Candidatus* Cloacimonas acidaminovorans str. Evry	25%/ 43%

Comparative genomics

Genome sequences of *M. cysteinexigens* B1-EB (NCBI accession AP018150.1), B2-EB (NCBI accession AP021872.1) and *M. cysteinexigens* AG77 (PATRIC accession 224135.3) were used for comparative genome analyses. The *M. cysteinexigens* AG77 genome was reorientated to start with *dnaA* (as for the other *Mycoavidus* genomes) and reannotated with Prokka 1.14.5.(16) Comparison of the three *Mycoavidus* genomes was performed using Roary v3.12.0 (17) with an 70 % protein identity cutoff. Genome synteny figures were constructed using Circos (18).

In general, evidence for the high dependence of these *Mycoavidus* symbionts on their hosts can be observed in the genomes. *M. cysteinexigens* AG77 has previously been found to be missing the biosynthetic pathway for the amino acid cysteine (19). Investigation of biosynthetic pathways in strain *Ca.* Mycoavidus necroximicus showed the loss of further amino acid biosynthesis pathways, including those for cysteine, histidine, isoleucine, leucine, methionine, threonine, tryptophan and tyrosine (https://papers.genomics.lbl.gov/cgi-bin/gapView.cgi) (20). This suggests that *Candidatus* Mycoavidus necroximicus relies very heavily on *M. verticillata* for the production of amino acid building blocks and might also explain why the fungus grows more aerial hyphae in the absence of endosymbionts. This is further reflected in the inability to grow *Candidatus* Mycoavidus necroximicus in an aposymbiotic manner, while axenic growth of *M. cysteinexigens* B1-EB^T, B2-EB and AG77 can be achieved by supplementing growth media with cysteine (5).

General analytical methods

Analytical HR-ESI-LC/MS. Exactive Orbitrap High Performance Benchtop LC/MS (Thermo Fisher Scientific) with an electron spray ion source and an Accela HPLC System, C18 column (Betasil C18, 150 × 2.1 mm, Thermo Fisher Scientific), solvents: acetonitrile and water (both supplemented with 0.1 % formic acid), flow rate: 0.2 mL min^{-1}; program: hold 1 min at 5 % acetonitrile, 1–16 min 5–98 % acetonitrile, hold 3 min 98 % acetonitrile, 19–20 min 98 % to 5 % acetonitrile, hold 3 min at 5 % acetonitrile.

MS/MS (tandem mass spectrometry). QExactive Orbitrap High Performance Benchtop LC/MS (ThermoFisher) with an electron spray ion source and an Accela HPLC System, C18 column (Accucore C18 2.6 µm, 100 × 2.1 mm, Thermo Fisher Scientific) and the following solvent system: acetonitrile and water (both supplemented with 0.1 % formic acid) at a flow rate of 0.2 mL min^{-1}; gradient: 0–10 min 5–98 % acetonitrile, hold 4 min 98 % acetonitrile, 14–14.1 min 98 % to 5 % acetonitrile, hold 6 min at 5 % acetonitrile.

NMR. 600 MHz Avance III Ultra Shield (Bruker) and signals were referenced to the residual solvent signal. ^{1}H 600 MHz, ^{13}C 150 MHz; NMR solvent: DMSO-d_6.

Optical rotation. Jasco P-1020 polarimeter, Na light (589 nm), at 25 °C, 50 mm cell length, c 2 w/v%, dissolved in 83% acetonitrile (83% MeCN).

Identification, extraction and isolation of secondary metabolites

Extraction of necroxime D (CJ-12,290) (4) and necroxime C (CJ-13,357) (3). *M. verticillata* NRRL 6337 was either cultivated in modified medium 2 (21) for 7 days, at 160 rpm and 26 °C or on PDA plates at 26 °C for 28 days (Table S 2). The cultures were extracted with 1:1 volume of ethyl acetate overnight. Following, the organic phase was concentrated under reduced pressure and the residue was dissolved in a small volume of methanol. The extracts were measured *via* LC/MS.
Measured *m/z* 459.1833 and 459.1758 $[M+H]^+$, calculated 459.1762, $C_{23}H_{27}N_2O_8$ (CJ-12,290/CJ-13,357; **4**/**3**)

Extraction of lassopeptide mycetohabin-15 (8). *M. verticillata* NRRL 6337 or *Burkholderia* sp. HKI-404 (strain B8) were cultivated in MM9 medium for 7 days, with orbital shaking at 160 rpm and 26 °C. The absorber resin XAD-2 was added for 30 min to the culture, followed by separation of the resin and extraction with 100 % methanol overnight. The organic phase was concentrated under reduced pressure and the residue was dissolved in a small volume of methanol. The extracts were measured *via* LC/MS.
Measured *m/z* 768.3931 $[M+2H]^{2+}$ (Mycetohabin-15; **8**)

Production of necroxime A (1). *Burkholderia* sp. strain B8 wild type or Δ*necA* mutant were cultivated in MGY+M9 medium for 4–5 days with orbital shaking at 110 rpm and 30 °C. Absorber resin XAD-2 was added to the bacterial culture for 30 min, separated from the culture and extracted in 100 % methanol for 4 hours. The organic phase was concentrated under reduced pressure and the residue was dissolved in a small volume of methanol. The extracts were measured *via* LC/MS.
Measured *m/z* 673.3088 $[M+H]^+$, calculated 673.3079, $C_{33}H_{45}N_4O_{11}$ (necroxime A; **1**)

Isolation of necroxime D (4) from *M. verticillata* NRRL 6337. Necroxime D (**4**) was the main metabolite detected in fresh extracts of the *Mycoavidus* endosymbionts with no prior light-exposure; as **4** then easily isomerizes into **3** under long-term light exposure (21), we isolated only species **4** (Figure S 7). The fungal host *M. verticillata* NRRL 6337 was cultivated on PDA plates at 26 °C for 28 days. The culture was extracted twice with 1:1 volume of ethyl acetate overnight. Following, the organic phase was concentrated under reduced pressure and the residue was dissolved in a small volume of methanol. The extract was pre-fractionated on an open Sephadex LH-20-column with methanol and the necroxime-containing fraction was further purified with a preparative HPLC under following conditions: A: H_2O + 0.01 % TFA, B: Methanol; 15–100 % B in 35 min, 15 mL min^{-1} (Phenomenex, Luna, 10 µm, C18(2), 100 Å, 250 × 21.2 mm).

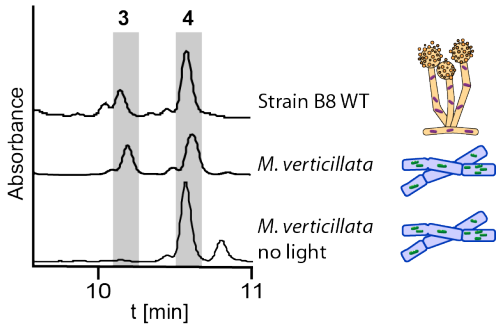

Figure S 7. Metabolic profiles of necroxime-containing extracts from *Burkholderia* sp. strain B8 and *M. verticillata* (cultivated and extracted under normal and light-reduced conditions).

Comparison of necroxime C and D (3 and 4) from *Burkholderia* sp. strain B8 and *M. verticillata* NRRL 6337. For the identification of the necroximes C and D from *M. verticillata* NRRL 6337 the previously described and isolated substances from *Burkholderia* sp. strain B8 were used as authentic standards (22). Co-injection revealed the same retention times of the substances isolated from the two producers. MS/MS fragmentation showed identical fragmentation patterns of the substances (Figure S 13–16). Comparison of the chemical shifts in NMR measurements of necroximes C and D (**3** and **4**) from *Burkholderia* sp. strain B8 and necroxime D (**4**) from *M. verticillata* revealed the identical configuration within the respective molecules (Table S 9). To unambiguously verify that the isolated necroximes from *Burkholderia* sp. strain B8 and *M. verticillata* NRRL 6337 are identical molecules and no enantiomers, we determined the optical rotation of necroxime C and D (**3** and **4**) isolated from *Burkholderia* sp. strain B8. The comparison of the measured values with the published values for necroxime C (CJ-13,357) (**3**) and necroxime D (CJ-12,290) (**4**) (21) identified the molecules to be the same, as a similar rotation can be measured (Table S 4). Additionally, we performed genome mining with the two BGCs from necroximes and CJ-compounds, extracted the ketoreductase domain sequences that determine the absolute configurations of the incorporated OH residues, and compared the specificity codes using Mega7 (23) and ClustalW (24). HXXXXXXD codes for D-β-OH as shown by Caffrey (25). That way we could determine the absolute configuration of the OH groups and, consequently, show that necroximes C–D are stereochemically identical to CJ-13,357 and CJ-12,950 (Figure S 8).

Table S 4. Comparison of optical rotation of necroxime C and D (3 and 4) isolated from *Burkholderia* sp. strain B8 and *M. verticillata* NRRL 6337.

	necroxime C (CJ-13,357) (**3**)	necroxime D (CJ-12,290) (**4**)
M. verticillata NRRL 6337 [α]D (25 °C, MeOH)	+ 107.8° (c 0.23)	+ 99.5° (c 0.22)
Burkholderia sp. strain B8 [α]D (25 °C, MeOH)	+ 89.9° (c 0.12)	+ 74.4° (c 0.25)

A

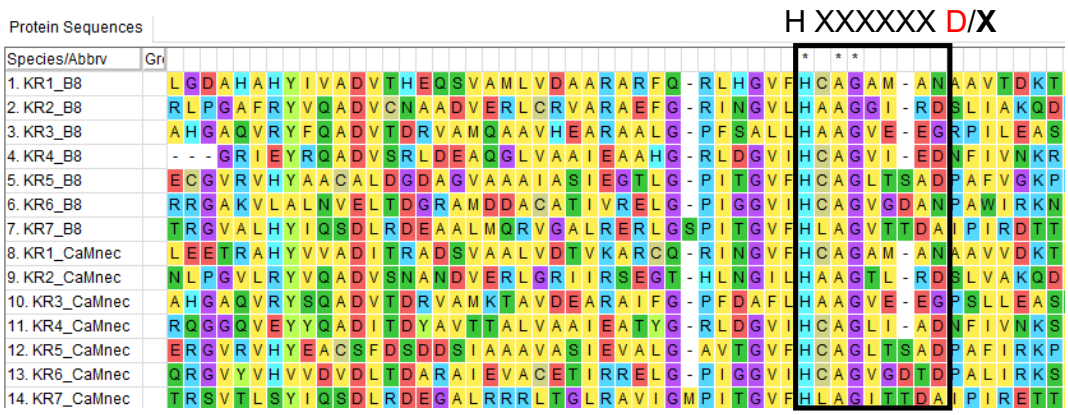

B

Organism	Module nr.	KR specificity code	Prediction
Mycetohabitans sp. strain B8	3	H CAGAMA **N**	L
Ca. M. necroximicus	3	H CAGAMA **N**	L
Mycetohabitans sp. strain B8	4	H AAGGIR **D**	**D**
Ca. M. necroximicus	4	H AAGTLR **D**	**D**
Mycetohabitans sp. strain B8	5	H AAGVEE **G**	L
Ca. M. necroximicus	5	H AAGVEE **G**	L
Mycetohabitans sp. strain B8	6	H AAGVIE **D**	**D**
Ca. M. necroximicus	6	H AAGLIA **D**	**D**
Mycetohabitans sp. strain B8	7	H CAGLTS **A**	L
Ca. M. necroximicus	7	H CAGLTS **A**	L
Mycetohabitans sp. strain B8	9	H CAGVGD **A**	L
Ca. M. necroximicus	9	H CAGVGD **T**	L
Mycetohabitans sp. strain B8	12	H LAGVTT **D**	**D**
Ca. M. necroximicus	12	H LAGITT **D**	**D**

Figure S 8. Multiple Sequence Alignment using KR domain sequences encoded in the necroxime BGCs of *Mycetohabitans* sp. strain B8 and *Ca.* Mycoavidus necroximicus unveils predicted configurations of OH groups in the natural products. A) Part of the alignment showing specificity code HXXXXXXD/X. B) Extracted specificity codes according to module architecture. Comparison of KR domain specificities extracted from strain B8 and *Ca.* Mycoavius necroximicus reveals identical L/D distibution.

Nematodal strains and cultivation conditions

The model organism *Caenorhabditis elegans* (*C. elegans* Genetics Centre (CGC, University of Minnesota, USA)) was maintained on *Escherichia coli* OP50 seeded on NGM agar (26). For culture maintenance a small, nematode-containing agar-piece of NGM was transferred onto fresh *E. coli*-covered NGM plates. Plates were kept at 20 °C for 4–7 days. *E. coli* OP50 was cultured in LB medium. If prepared for an assay, nematodes were washed from the plates with K-medium and left for settling at 4 °C for 30 min. Supernatant was discarded and resuspended in 8 mL K-medium for usage in experiments.

The nematode *Aphelenchus avenae* was obtained as a kind gift from Prof. Dr. Markus Künzler (ETH Zürich) and kept on a sporulation-deficient *Botrytis cinerea* strain (BC-3), grown on malt extract agar (MEA) containing 100 µg mL^{-1} chloramphenicol at 21 °C. Harvest of nematodes was performed via Baermann funneling as described earlier, with small variations (27). Nematode-containing plates were cut into small pieces and left upside-down overnight in a funnel lined with miracloth (Merck) and filled with K-medium. After release of the funnel, nematodes were sterilized for two hours in K-medium containing 100 mM geneticin (G418) and 25 µg mL^{-1} kanamycin, washed once with K-medium and plated onto 1.5 % agar plates containing 200 mM geneticin and 50 µg mL^{-1} kanamycin. After 24–40 h of sterilization and starvation, *A. aphelenchus* were washed from plates with K-medium and transferred onto fungi.

Nematode bioassays

***C. elegans* liquid assay.** Liquid assays for active-fraction determination and potency assessment were conducted as previously described (28). In short, *E. coli* was grown in 50 mL LB medium overnight, with orbital shaking at 150 rpm. Cells were pelleted and resuspended in K-medium. OD_{600} was measured and cells diluted to OD_{600} 1.2. An *E. coli* suspension (1.76 mL) was transferred to each well, supplemented with 200 µL nematode suspension and 40 µL test substance resuspended in MeOH. For fraction-testing cured and symbiotic *M. verticillata* NRRL6337 cultures, grown for 16 days on 400 mL PDA, were extracted with ethyl acetate as described above. The extract was fractionated using a preparative HPLC under following conditions: A: H_2O + 0.01 % TFA, B: methanol; 15 % B for 5 min, 15–100 % B in 35 min, 100 % B for 10 min, 15 mL min^{-1} (Phenomenex, Luna, 10 µm, C18(2), 100 Å, 250 × 21.2 mm). Eight fractions were collected (every 5 min one fraction) with an additional fraction at 100 % B for 10 min. The fractions were dried in vacuum and resuspended in 1 mL MeOH. For potency assessment pure **4**, dissolved in MeOH was tested in following concentrations: 0.1 µg mL^{-1}, 0.3 µg mL^{-1}, 1 µg mL^{-1}, 3 µg mL^{-1}, 10 µg mL^{-1}, 30 µg mL^{-1}, 100 µg mL^{-1} and 300 µg mL^{-1}. The nematode suspension was prepared as described above. The OD_{600} of each well was measured at the start of the experiment and compared to the OD_{600} after 4 days of incubation at 20 °C and orbital shaking at 50 rpm. Methanol, 18 mM boric acid (dissolved in H_2O) and K-medium were used as controls for substance activity and a well without nematodes was used as a control for natural degradation-control of the bacteria. All steps were carried out under sterile conditions. For IC_{50} calculation GraphPad Prism 8 was used. The OD_{600} after 4 days of incubation with pure Methanol was used as an infinite small concentration of necroxime, whereas an infinite high concentration was set to 100 % starting OD_{600} *E. coli* (comparable with *E. coli* control).
The results of three biological replicates with each three technical replicates were analyzed for fraction assessment, whereas five biological replicates with three technical replicates each were used for potency determination of necroxime D (**4**).

***A. avenae* co-incubation assay.** A small amount of hyphae of each tested *Mortierella* strain was transferred to a PDA plate and incubated at 24 °C overnight. Nematodes from one plate were sterilized and starved as described above. After one washing step, nematodes were resuspended in 300 µL K-medium and aliquots of 50 µL were distributed onto the fresh fungal cultures. Plates were dried and controlled for living nematodes, before they were incubated for 17–24 days at 20 °C. For the evaluation, nematodes were harvested via Baermann funneling as described above. Funneled *A. avenae* were recovered on 1.5 % agar plates containing 200 mM geneticin and 50 µg mL^{-1} kanamycin overnight and subsequently investigated with a Zeiss Axio Zoom.V16 Stereomicroscope (Zeiss, Oberkochen, Germany) and a magnitude of 25 (Figure S 9). For plates with expected high nematode numbers, only a quarter was transferred onto the agar plates and the actual nematode number recalculated. The number of nematodes on the first frame of each video was counted manually. The mean of the cured *M. verticillata* NRRL 6337 cultures was set to 100 % for each biological replicate and the numbers of the other co-cultivations were calculated in relation to these 100 % (Table S 5). For statistical evaluation and significance evaluation a two-way analysis of variance followed by Tukey's multiple comparisons test with GraphPad Prism 8 was performed (Table S 6). Time series were bioinformatically analyzed as described later. Remaining plates were extracted with ethyl acetate to control the metabolite production. All steps were carried out under sterile conditions. The results of three biological replicates with each three technical replicates were used for analysis.

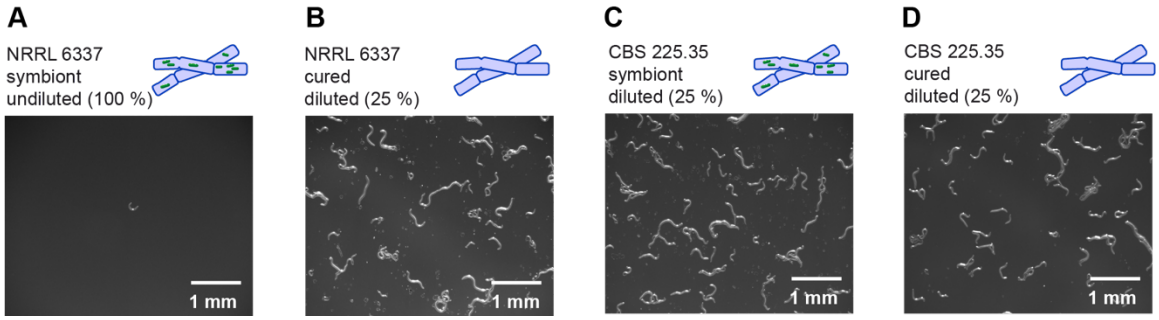

Figure S 9. Exemplary images of harvested nematodes from diverse co-cultivations with a magnification of 25 ×. A) Nematodes grown on symbiotic *M. verticillata* NRRL 6337. Sample of nematodes was undiluted. B) Nematodes of co-culture with a cured *M. verticillata* NRRL 6337. Sample of nematodes represent one quarter of the total nematode count, harvested from the co-incubation. C) Nematodes of co-culture with a symbiotic *M. verticillata* CBS 225.35. Sample of nematodes represent one quarter of the total nematode count, harvested from the co-incubation. D) Nematodes of co-culture with a cured *M. verticillata* CBS 225.35. Sample of nematodes represent one quarter of the total nematode count, harvested from the co-incubation.

Table S 5. Relative numbers of nematodes washed out of *Mortierella* and *A. avenae* co-cultures. Numbers correspond to nematode-counts for each technical replicate from a stereomicroscopic frame with a magnitude of 25. Mean of absolute nematode counts from NRRL 6337 cured were set to 100 % for each biological replicate and relative numbers were calculated based on corresponding 100 %.

Fungal strain	Biological replicate 1 Relative nematode numbers [%]			Biological replicate 2 Relative nematode numbers [%]			Biological replicate 3 Relative nematode numbers [%]		
NRRL 6337 symbiont	17.500	5.000	7.500	0.329	0.658	0.329	1.148	1.913	0.765
NRRL 6337 cured	107.500	120.000	72.500	69.737	152.632	77.632	122.449	113.265	64.286
CBS 225.35 symbiont	155.000	117.500	207.500	128.947	119.737	110.526	52.041	56.633	58.163
CBS 225.35 cured	250.000	187.500	77.500	31.579	26.316	121.053	45.918	73.469	75.000

Table S 6. Results of the statistical analysis (two-way analysis of variance and Turkey's multiple comparison test) representing the significant differences in nematode-counts of the tested co-cultures.

Turkey's multiple comparison test	Mean difference	95 % Confidence interval of difference	Adjusted *p* value	Significance
NRRL 6337 symbiont vs. NRRL 6337 cured	–96.10	–128.1 to –63.5	<0.0001	****
NRRL 6337 symbiont vs. CBS 225.35 symbiont	–107.90	–159.3 to –56.5	0.0007	***
NRRL 6337 symbiont vs. CBS 225.35 cured	–94.80	–170.5 to –19.1	0.0164	*
NRRL 6337 cured vs. CBS 225.35 symbiont	–11.78	–80.5 to 56.9	0.9441	ns
NRRL 6337 cured vs. CBS 225.35 cured	1.30	–84.5 to 87.1	>0.9999	ns
CBS 225.35 symbiont vs. CBS 225.35 cured	13.08	–69.8 to 95.9	0.9555	ns

Image analysis and mathematical modeling of *A. avenae* viability in fungal-nematodal co-incubations. Time series from *A. avenae* co-incubation assay were further analyzed regarding the mobility ratios of the nematodes, which could be harvested from the co-incubation assays. The native Zeiss format CZI files of the nematode samples were analyzed using the 25 × magnification subset of images. This magnification provided a suitable number of observed nematodes per field of view to assure that proper statistical analysis of the kinetic studies could be carried out, whilst maintaining an optical resolution that allowed for precise analysis of the individual nematodes' morphology. The image analysis was carried out using a Fiji (29) macro (ImageJ 1.52s and 1.53c, (30)), modified from our previously established ACAQ-v3 platform (31) to suit the current study. The tracking of the nematodes and further analyses were carried out by our newly developed JIPipe platform (https://www.jipipe.org/). Briefly: the raw CZI images were imported into memory; they were then sharpened, followed by Hessian filtering using the FeatureJ plugin from ImageJ (https://imagescience.org/meijering/software/featurej), where the smallest Hessian eigenvalue images were blurred with a Gaussian filter of 2 pixel radius using a disk element. These images were then thresholded according to the Li algorithm in ImageJ, followed by a closing morphological operator using 2 pixel radius disk elements, as provided by the MorphoLibJ plugin of ImageJ (32). The non-nematode elements of the images were eliminated by applying the Remove Outliers command of ImageJ, first with a radius of 5 pixels, then with 10 pixels; the threshold value was always 50. The clustered objects were separated by applying the watershed algorithm, followed by 2-pixel erosion. The segmented time-series images of nematodes were then loaded into a JIPipe workflow, where the individual nematodes were tracked in time using the "Split into connected components" node. The workflow was then forked; one branch was used to extract the track elements per time point per nematode, whereas the parallel branch summed up the total area covered by each individual nematode during the complete observation time. The ratio between a nematode's area and the total area covered by the same nematode during the entire time series was then used for further analysis. Here, when a nematode was motionless during the entire time series, this ratio would equal one, whereas a fast-moving nematode would be characterized by a high value of this ratio. The faster the nematode's movement, the higher the ratio. The time series of values was further processed to calculate its mean and standard deviation in order to characterize each track in terms of the underlying nematode's health status. We defined that a "dead or paralyzed" nematode would result in a ratio between 1.0 and 1.39 for its track, whereas a "live" nematode would have a ratio above 1.4 (Figure S 10). All results were saved in CSV file formats for further analysis.

When comparing the mobility ratios of the nematodes based on the method described above, the effect sizes using Hedges' g and Cohen's d were calculated for each pair of conditions, using the Effect Size Calculator from Social Science Statistics (www.socscistatistics.com) (Table S 7 and S 8). Typically, effect sizes below 0.2 are considered to indicate a trivial difference, whereas values above 0.8 indicate a real difference between the compared distributions.

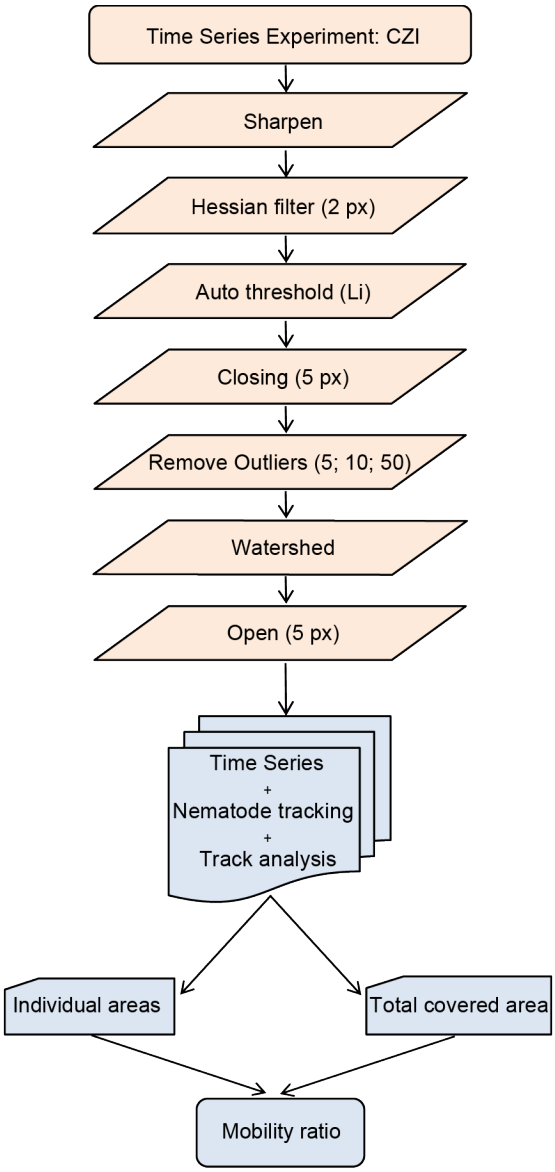

Figure S 10**.** Exemplified steps during image analysis and mathematical modeling of experiments regarding *A. avenae* viability in fungal-nematodal co-incubations.

Table S 7. Overview of analyzed of the different fungal-nematodal co-cultivations with mean numbers in percent of live nematodes and corresponding standard deviation.

Fungal strain	Analyzed	Mean value alive [%]	Standard deviation of mean value [%]
NRRL 6337 symbiont	238	33.7	28.0
NRRL 6337 cured	487	61.9	9.7
CBS 225.35 symbiont	176	63.2	3.2
CBS 225.35 cured	568	73.9	17.2

Table S 8. Effect size calculations for the mobility ratios of the different fungal-nematodal co-cultivations.

Compared populations	Hedges' *g*	Cohen's *d*	Strength of effect
NRRL 6337 symbiont vs. NRRL 6337 cured	1.58	1.35	Very large
NRRL 6337 symbiont vs. CBS 225.35 symbiont	1.38	1.48	Very large
NRRL 6337 symbiont vs. CBS 225.35 cured	1.92	1.73	Very large
NRRL 6337 cured vs. CBS 225.35 symbiont	0.15	0.18	Very small
NRRL 6337 cured vs. CBS 225.35 cured	0.84	0.86	Moderate
CBS 225.35 symbiont vs. CBS 225.35 cured	0.71	0.86	Moderate

***A. avenae* chemical complementation assay.** A small amount of hyphae of cured or symbiotic *M. verticillata* NRRL 6337 strains was transferred onto 1 mL PDA filled into 12-well plates and incubated overnight at 26 °C. On cultures inoculated for chemical complementation 11.4 µg (25 µM), 22.8 µg (50 µM), 50 µg (109 µM) or 100 µg (219 µM) necroxime D (**4**) dissolved in 200 µL 50 % MeOH were applied and dried under sterile conditions. Control cultures were overlaid with 200 µL 50 % MeOH and dried. Aliquots of 50 µL nematode suspension, prepared as described above, were distributed onto fungi, dried and co-incubated for 14 days at 20 °C. For evaluation, co-culture was removed from the wells and washed in 5 mL K-medium overnight. Medium including the washed nematodes was filtered through miracloth (Merck) to avoid agar carry-over and left at 4 °C for 1 h to let nematode settle. Supernatant was discarded and remaining nematodes transferred onto 6-well plates containing 5 mL 1.5 % agar plates with 200 mM geneticin and 50 µg mL^{-1} kanamycin. After plates were dried under sterile conditions, the amount of harvested nematodes from each plate was assessed with a Zeiss Axio Zoom V16 Stereomicroscope (Zeiss, Oberkochen, Germany) (three biological replicates with each three technical replicates) (Figure S 11 and S 12).

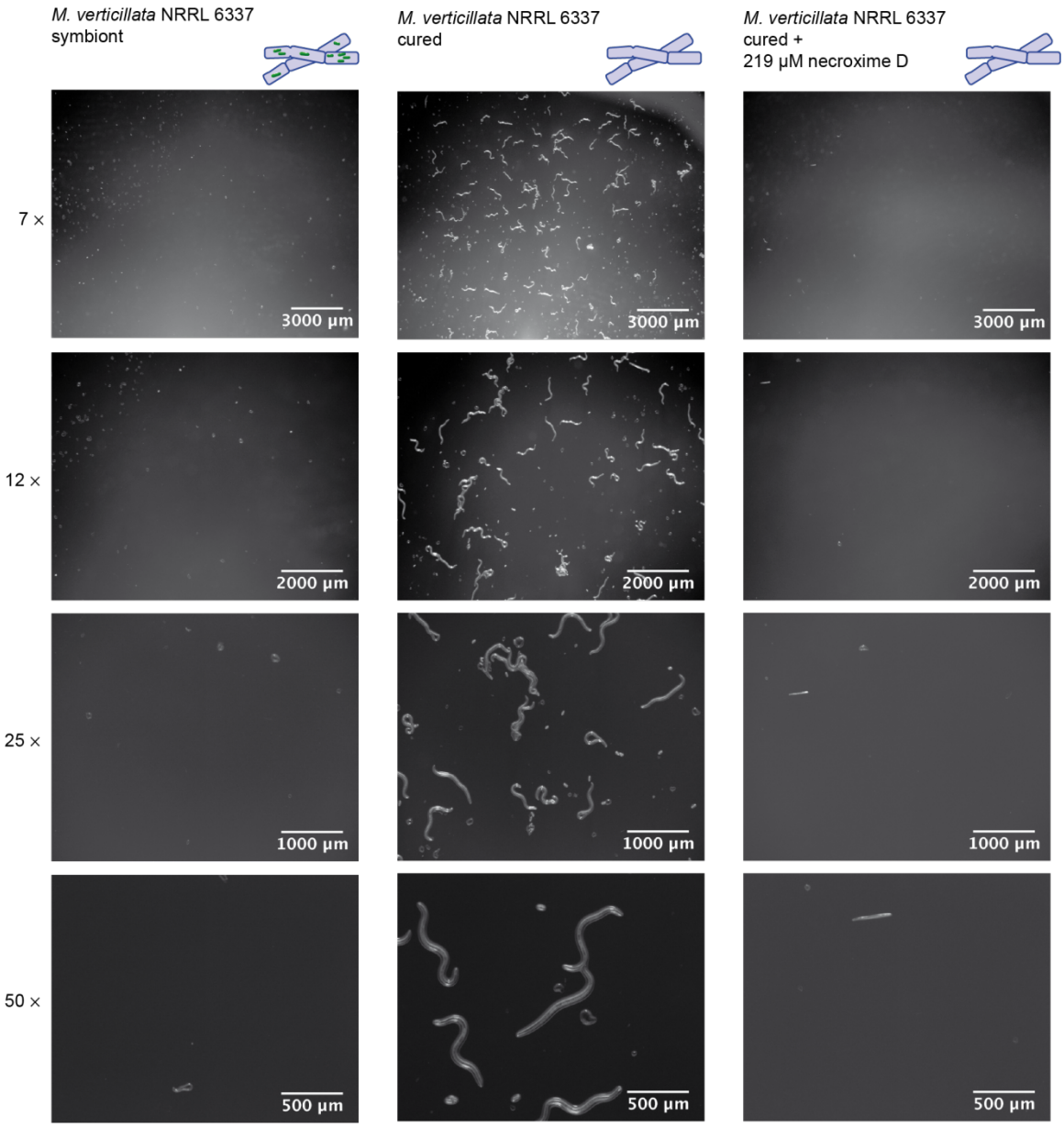

Figure S 11. Stereomicroscopy images in various magnifications of *A. avenae* harvested from symbiotic *M. verticillata* NRRL 6337 cultures, cured *M. verticillata* NRRL 6337 cultures and cured *M. verticillata* NRRL 6337 cultures complemented with 219 µM necroxime D (**4**).

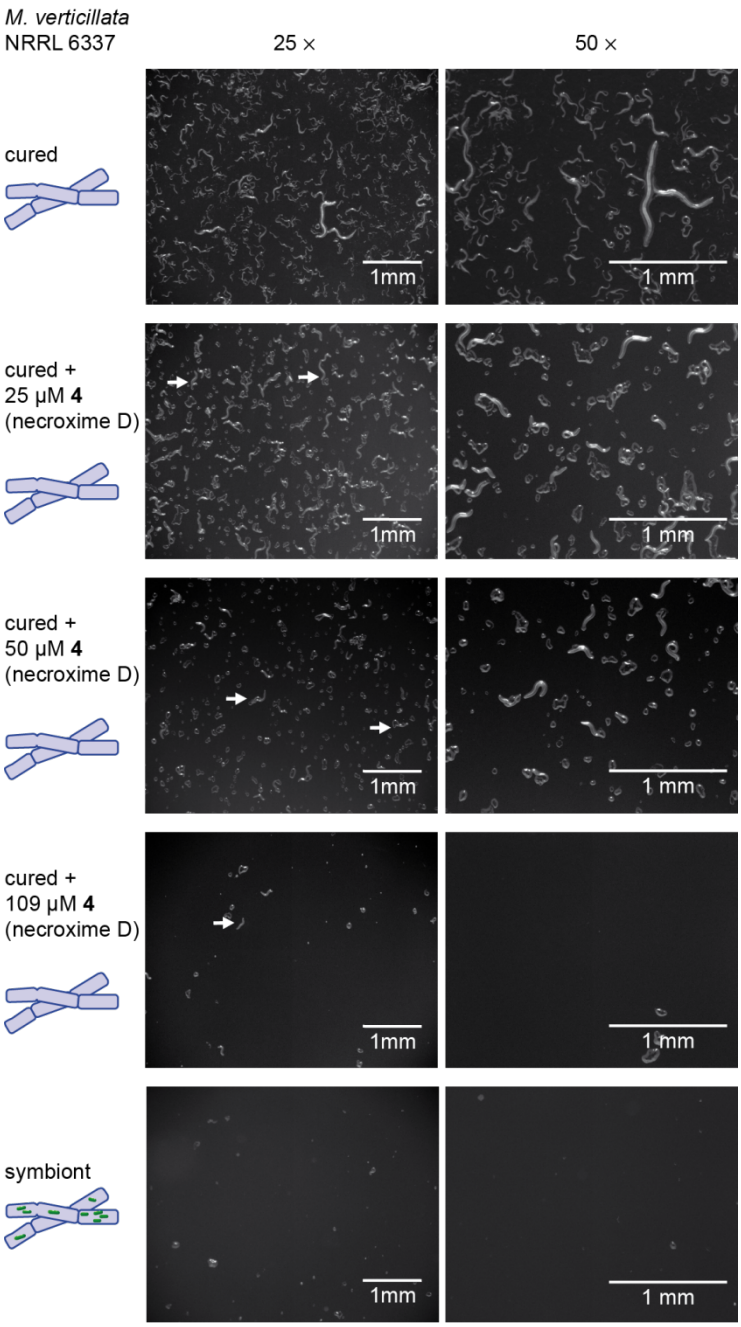

Figure S 12. Stereomicroscopy images in two magnifications of *A. avenae* harvested from symbiotic *M. verticillata* NRRL 6337 cultures, cured *M. verticillata* NRRL 6337 cultures and cured *M. verticillata* NRRL 6337 cultures complemented with 25 µM, 50 µM and 109 µM necroxime D (**4**). White arrows indicate nematodes beside same-sized agar pieces.

MS/MS and NMR data

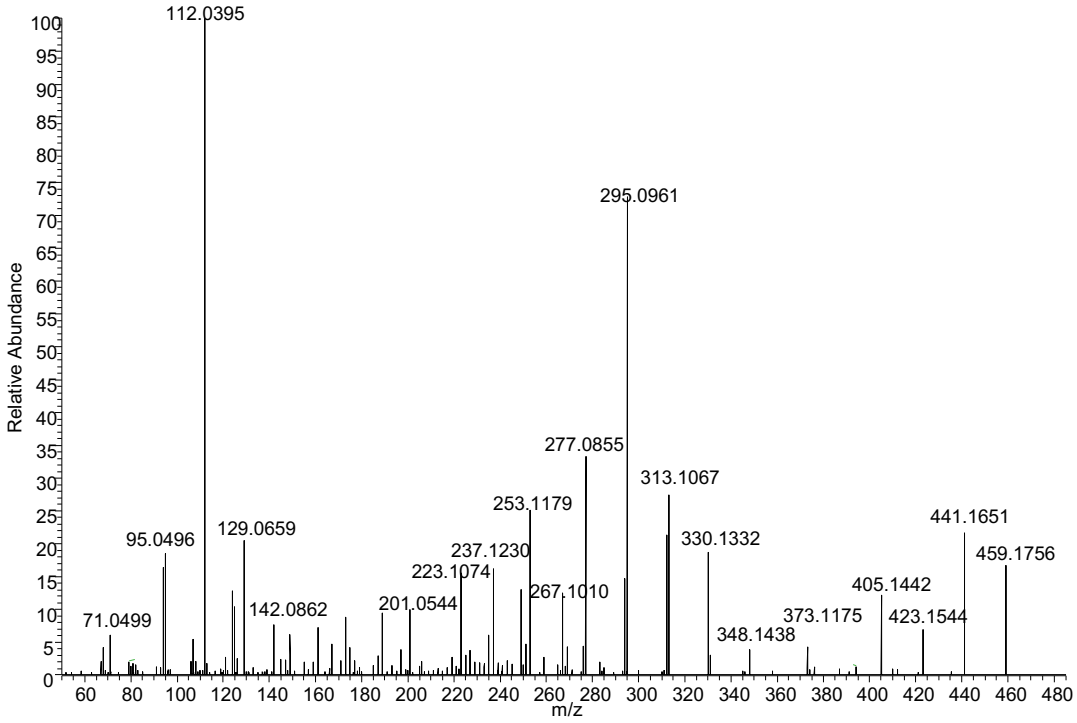

Figure S 13. MS/MS fragmentation pattern of *m/z* 459.1756 [*M*+H]$^+$ (necroxime C, **3**) in *Burkholderia* sp. strain B8 cultures.

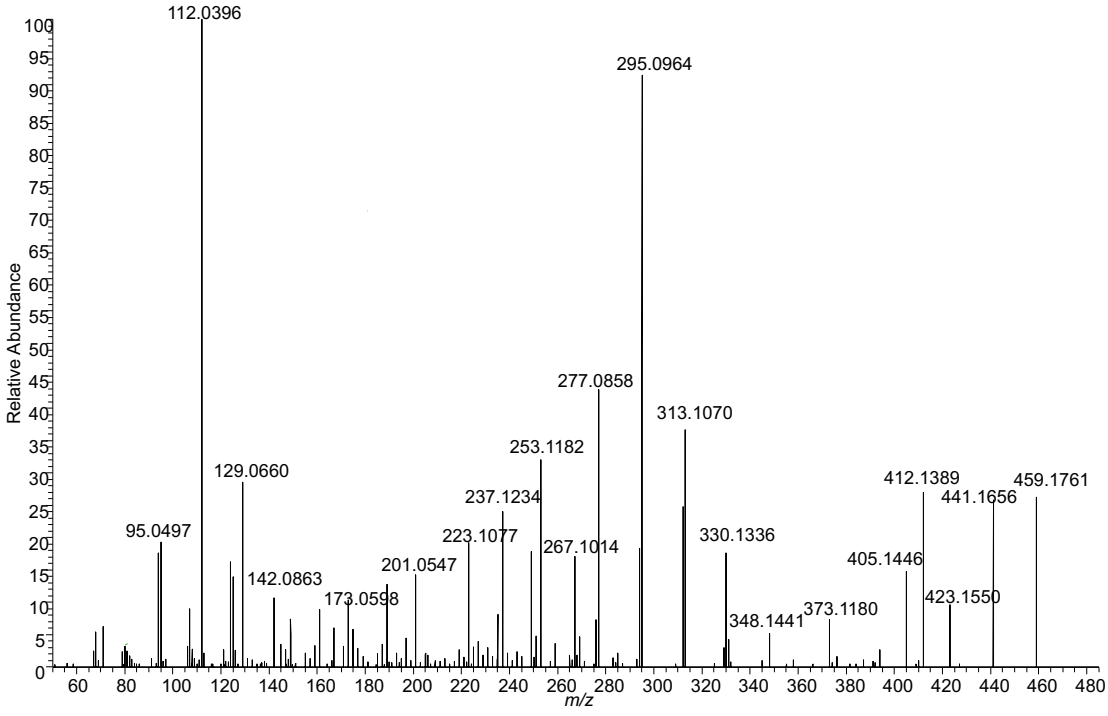

Figure S 14. MS/MS fragmentation pattern of *m/z* 459.1756 [*M*+H]$^+$ (CJ-13,357, **3**) in *M. verticillata* NRRL 6337 cultures.

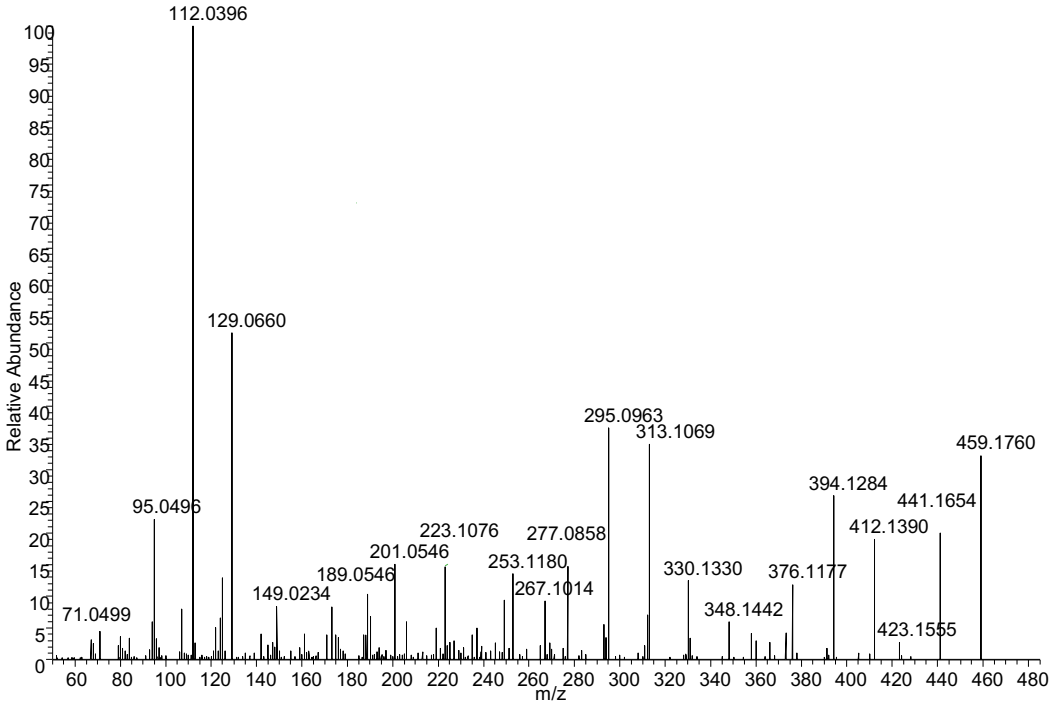

Figure S 15. MS/MS fragmentation pattern of *m/z* 459.1760 [*M*+H]$^+$ (necroxime D, **4**) in *Burkholderia* sp. strain B8 cultures.

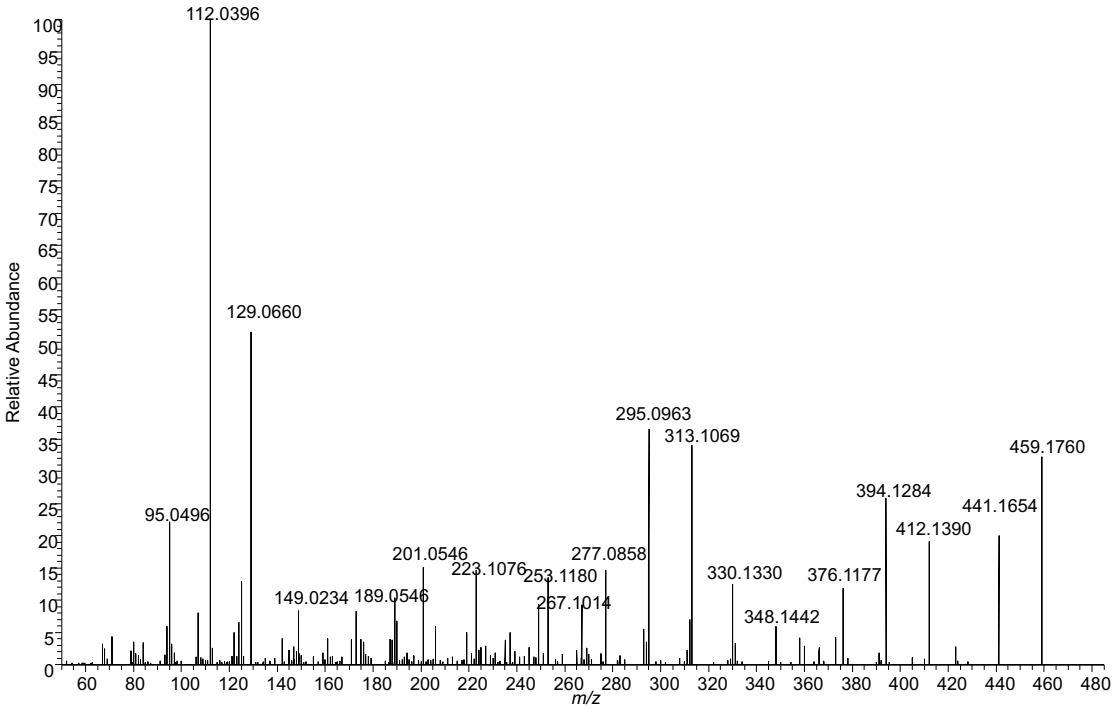

Figure S 16. MS/MS fragmentation pattern of *m/z* 459.1756 [*M*+H]$^+$ (CJ-12,950, **4**) in *M. verticillata* NRRL 6337 cultures.

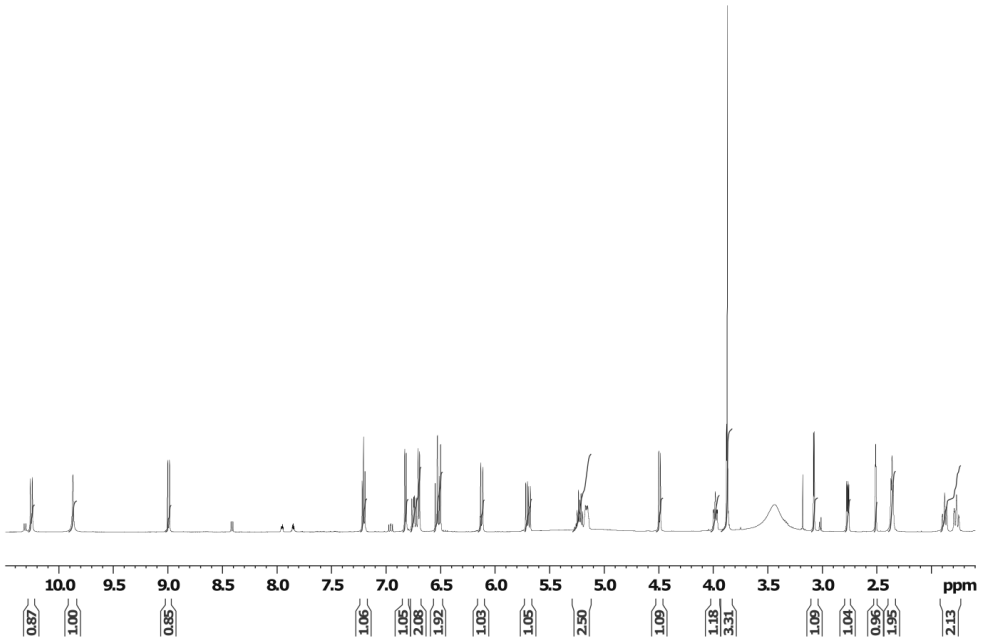

Figure S 17. ^{1}H-NMR of necroxime D (**4**) isolated from *M. verticillata* NRRL 6337 cultures.

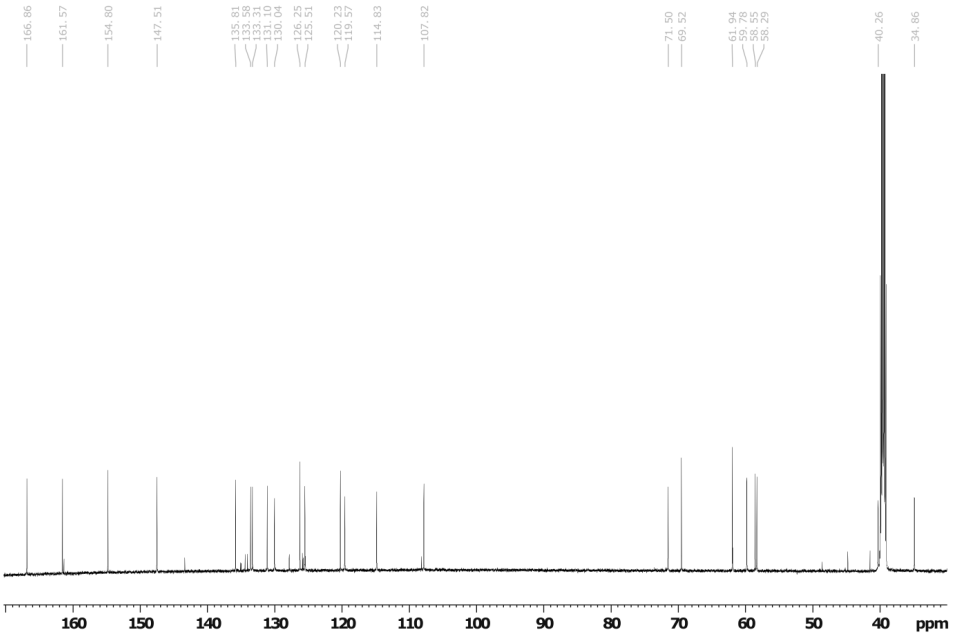

Figure S 18. ^{13}C-NMR of necroxime D (**4**) isolated from *M. verticillata* NRRL 6337 cultures.

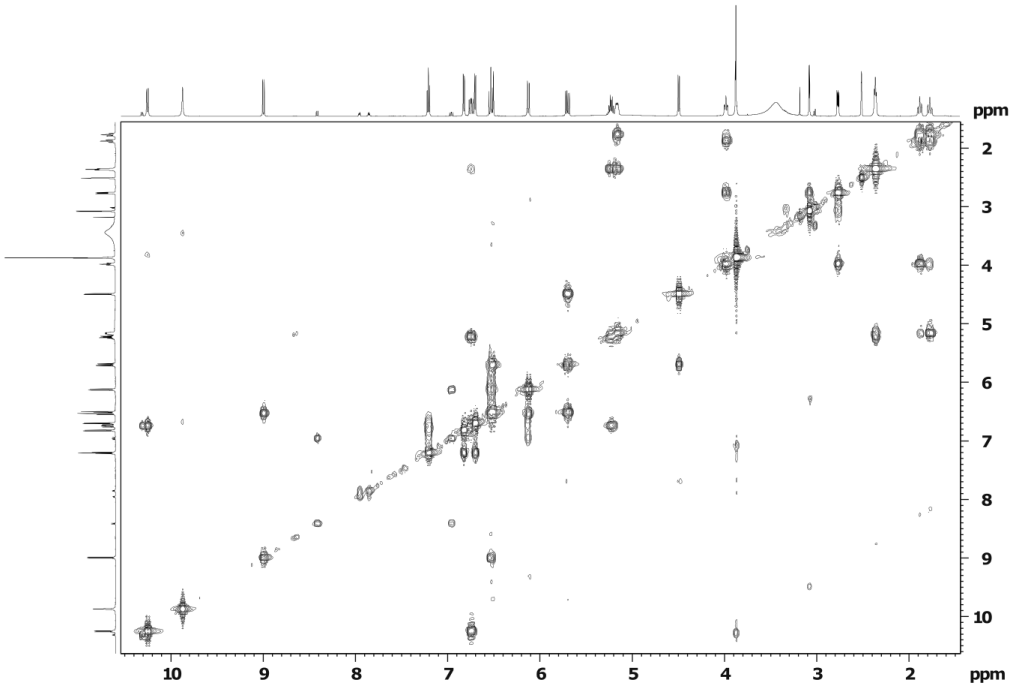

Figure S 19. ^{1}H-^{1}H-COSY-NMR of necroxime D (**4**) isolated from *M. verticillata* NRRL 6337 cultures.

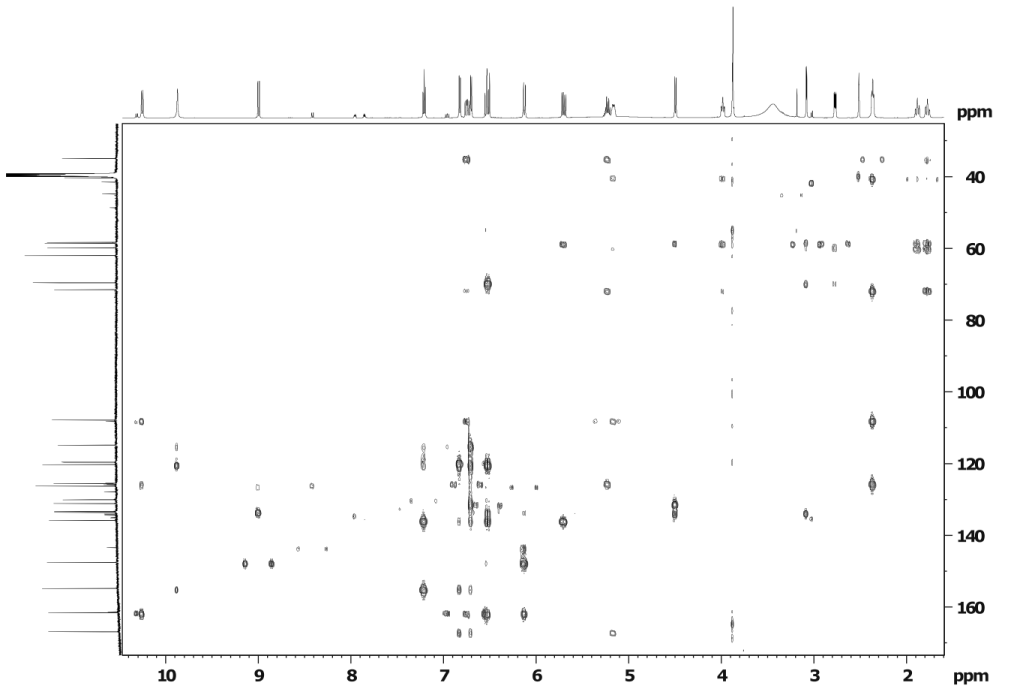

Figure S 20. ^{1}H-^{13}C-HMBC-NMR of necroxime D (**4**) isolated from *M. verticillata* NRRL 6337 cultures.

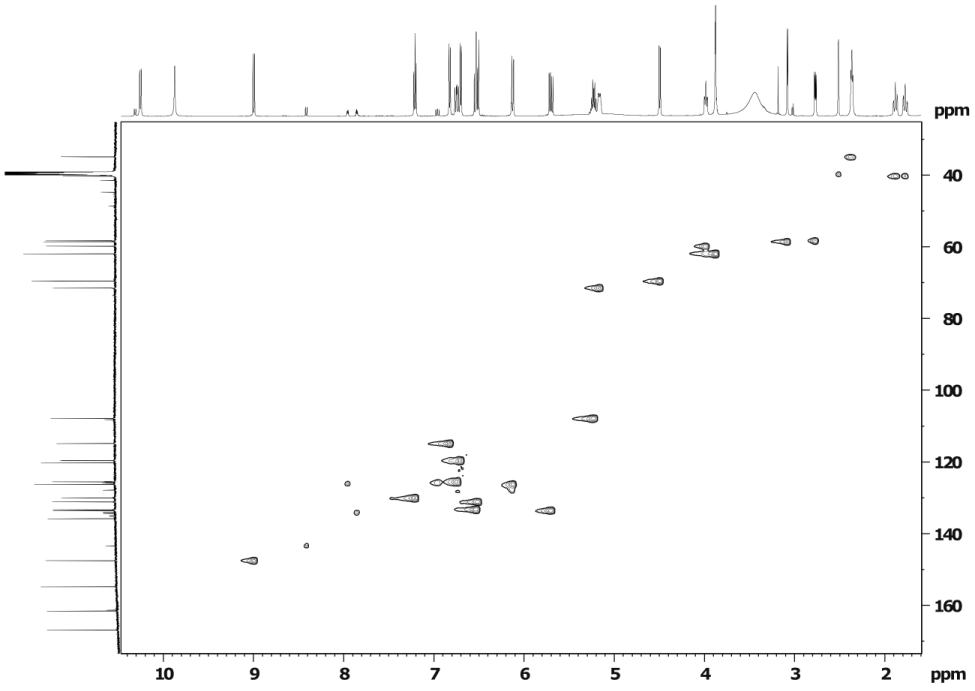

Figure S 21**.** ^{1}H-^{13}C-HSQC-NMR of necroxime D (**4**) isolated from *M. verticillata* NRRL 6337 cultures.

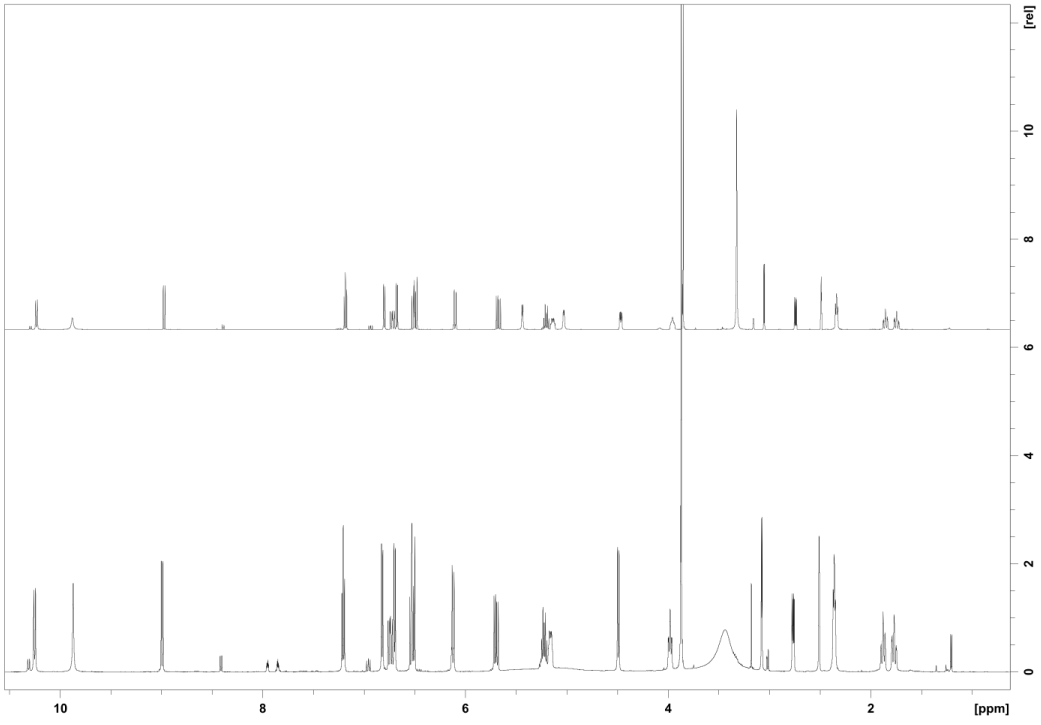

Figure S 22. Comparison of ^{1}H-NMR of necroxime D (**4**) isolated from *M. verticillata* NRRL 6337 cultures and ^{1}H-NMR of necroxime D (**4**) isolated from *Burkholderia* sp. strain B8 cultures.

Table S 9. Comparison of the chemical shifts from the NMR data of necroxime D (CJ-12,950, **4**) isolated from *M. verticillata* NRRL 6337 cultures and NMR data of necroxime C and D (**3** and **4**) isolated from *Burkholderia* sp. strain B8 cultures. Main differences between *E*/*Z* isomers are marked in red.

	Necroxime C (3)		**Necroxime D (4)**		**CJ-12,950 (4)**	
Pos.	δ_C [ppm]	δ_H [ppm]; Signal (*J* [Hz])	δ_C [ppm]	δ_H [ppm]; Signal (*J* [Hz])	δ_C [ppm]	δ_H [ppm]; Signal (*J* [Hz])
1	167.0	-	166.8	-	166.9	-
2	120.3	-	120.2	-	120.2	-
3	154.9	-	154.8	-	154.7	-
4	119.5	6.81; 1 H d (*8.0*)	114.8	6.80; 1 H d (*8.2*)	114.9	6.82; 1 H d (*8.6*)
5	130.0	7.20; 1 H t (*7.8*)	130.0	7.18; 1 H t (*8.0*)	130.0	7.21; 1 H t (*7.9*)
6	120.2	6.69; 1 H d (*7.4*)	119.5	6.68; 1 H d (*7.5*)	119.6	6.69; 1 H d (*7.6*)
7	135.8	-	135.8	-	135.8	-
8	131.1	6.51; 1 H d (*16.5*)	131.1	6.49; 1 H d (*16.2*)	131.1	6.51; 1 H d (*16.6*)
9	133.7	5.69; 1 H dd (*9.2; 16.4*)	133.6	5.67; 1 H dd (*9.2; 16.9*)	133.8	5.70; 1 H dd (*9.2; 16.2*)
10	69.5	4.49; 1 H dd (*4.2; 9.2*)	69.5	4.47; 1 H dd (*4.7; 9.1*)	69.5	4.49; 1 H d (*9.0*)
11	58.6	3.07; 1 H d (*4.3*)	58.5	3.05; 1 H d (*4.3*)	58.5	3.07; 1 H d (*4.2*)
12	58.3	2.76; 1 H dd (*4.2; 8.7*)	58.3	2.74; 1 H dd (*4.2; 8.5*)	58.2	2.77; 1 H dd (*4.1; 8.7*)
13	59.9	3.97; 1 H m	59.8	3.96; 1 H m	59.8	3.98; 1 H m
14	40.3	1.87; 1 H m	40.3	1.86; 1 H m	40.3	1.88; 1 H m
		1.77; 1 H m		1.74; 1 H m		1.76; 1 H m
15	71.5	5.15; 1 H m	71.5	5.14; 1 H m	71.5	5.16; 1 H m
16	34.7	2.35; 2 H t (*6.8*)	34.9	2.34; 2 H t (*7.1*)	34.9	2.36; 2 H t (*6.7*)
17	107.3	5.24; 1 H dt (*8.0; 14.5*)	107.8	5.20; 1 H dt (*7.0; 14.2*)	107.9	5.22; 1 H dt (*14.2; 7.2*)
18	125.5	6.76; 1 H dd (*10.3; 14.5*)	125.5	6.72; 1 H dd (*10.4; 14.4*)	125.5	6.75; 1 H dd (*10.2; 14.5*)
NH	-	10.23; 1 H d (*10.2*)	-	10.23; 1 H d (*10.3*)	-	10.25 1 H d (*10.1*)
19	161.3	-	161.6	-	161.6	-
20	130.5	6.39; 1 H d (*15.3*)	126.2	6.10; 1 H d (*11.6*)	126.2	6.12; 1 H d (*11.5*)
21	132.8	7.00; 1 H dd (*10.2; 15.5*)	133.3	6.52; 1 H dd (*10.2; 11.3*)	133.3	6.53; 1 H m
22	148.9	8.05; 1 H d (*10.6*)	147.5	8.97; 1 H d (*10.5*)	147.5	8.99 1 H d (*10.3*)
23	62.0	3.88; 3 H s	61.9	3.85; 3 H s	61.9	3.87; 3 H s
3-OH	-	9.86; 1 H br	-	9.88; 1 H br		9.87 1 H br
10-OH	-	5.46; 1 H br	-	5.44; 1 H d (*5.3*)		-

Legends for Movies

Movie S 1. *A. avenae* harvested from a co-culture with symbiotic *M. verticillata* NRRL 6337.

Movie S 2. *A. avenae* harvested from a co-culture with cured *M. verticillata* NRRL 6337.

SI References

1. P. Estrada-de los Santos *et al.*, Whole genome analyses suggests that *Burkholderia* sensu lato contains two additional novel genera (*Mycetohabitans* gen. nov., and *Trinickia* gen. nov.): implications for the evolution of diazotrophy and nodulation in the Burkholderiaceae. *Genes* **9**, 389 (2018).
2. F. Madeira *et al.*, The EMBL-EBI search and sequence analysis tools APIs in 2019. *Nucleic Acids Res.* **47**, W636-W641 (2019).
3. J. Trifinopoulos, L. T. Nguyen, A. von Haeseler, B. Q. Minh, W-IQ-TREE: a fast online phylogenetic tool for maximum likelihood analysis. *Nucleic Acids Res.* **44**, W232-235 (2016).
4. Y. Takashima *et al.*, Prevalence and intra-family phylogenetic divergence of *Burkholderiaceae*-related endobacteria associated with species of *Mortierella*. *Microbes Environ.* **33**, 417-427 (2018).
5. S. Ohshima *et al.*, *Mycoavidus cysteinexigens* gen. nov., sp. nov., an endohyphal bacterium isolated from a soil isolate of the fungus *Mortierella elongata*. *Int. J. Syst. Evol. Microbiol.* **66**, 2052-2057 (2016).
6. R. R. Wick, L. M. Judd, C. L. Gorrie, K. E. Holt, Unicycler: resolving bacterial genome assemblies from short and long sequencing reads. *PLoS Comput. Bio.* **13**, e1005595 (2017).
7. R. R. Wick, L. M. Judd, C. L. Gorrie, K. E. Holt, Completing bacterial genome assemblies with multiplex MinION sequencing. *Microb. Genom.* **3**, e000132 (2017).
8. K. Blin *et al.*, antiSMASH 5.0: updates to the secondary metabolite genome mining pipeline. *Nucleic Acids Res.* (2019).
9. G. Bashiri, A. M. Rehan, D. R. Greenwood, J. M. Dickson, E. N. Baker, Metabolic engineering of cofactor F420 production in *Mycobacterium smegmatis*. *PLoS One* **5**, e15803 (2010).
10. D. Braga *et al.*, Metabolic pathway rerouting in *Paraburkholderia rhizoxinica* evolved long-overlooked derivatives of coenzyme F420. *ACS Chem. Biol.* **14**, 2088-2094 (2019).
11. L. D. Eirich, G. D. Vogels, R. S. Wolfe, Proposed structure for coenzyme F420 from *Methanobacterium*. *Biochemistry* **17**, 4583-4593 (1978).
12. B. O. Bachmann, J. Ravel, Methods for *in silico* prediction of microbial polyketide and nonribosomal peptide biosynthetic pathways from DNA sequence data. *Methods Enzymol.* **458**, 181-217 (2009).
13. J. Uehling *et al.*, Comparative genomics of *Mortierella elongata* and its bacterial endosymbiont *Mycoavidus cysteinexigens*. *Environ. Microbiol.* **19**, 2964-2983 (2017).
14. Y. Guo *et al.*, *Mycoavidus* sp. Strain B2-EB: comparative genomics reveals minimal genomic features required by a cultivable Burkholderiaceae-related endofungal bacterium. *Appl. Environ. Microbiol.* **86**, e01018-01020 (2020).
15. D. Sharmin *et al.*, Comparative genomic insights into endofungal lifestyles of two bacterial endosymbionts, *Mycoavidus cysteinexigens* and *Burkholderia rhizoxinica*. *Microbes Environ.*, ME17138 (2018).
16. T. Seemann, Prokka: rapid prokaryotic genome annotation. *Bioinformatics* **30**, 2068-2069 (2014).
17. A. J. Page *et al.*, Roary: rapid large-scale prokaryote pan genome analysis. *Bioinformatics* **31**, 3691-3693 (2015).
18. M. Krzywinski *et al.*, Circos: an information aesthetic for comparative genomics. *Genome Res.* **19**, 1639-1645 (2009).
19. J. Uehling *et al.*, Comparative genomics of *Mortierella elongata* and its bacterial endosymbiont *Mycoavidus cysteinexigens*. *Environ. Microbiol.* **19**, 2964-2983 (2017).
20. M. N. Price, A. M. Deutschbauer, A. P. Arkin, GapMind: Automated Annotation of Amino Acid Biosynthesis. *mSystems* **5**, e00291-00220 (2020).
21. K. A. Dekker *et al.*, Novel lactone compounds from *Mortierella verticillata* that induce the human low density lipoprotein receptor gene: Fermentation, isolation, structural elucidation and biological activities. *J. Antibiot.* **51**, 14-20 (1998).

22. S. P. Niehs *et al.*, Mining symbionts of a spider-transmitted fungus illuminates uncharted biosynthetic pathways to cytotoxic benzolactones. *Angew. Chem. Int. Ed.* **59**, 7766-7771 (2020).
23. S. Kumar, G. Stecher, K. Tamura, MEGA7: Molecular Evolutionary Genetics Analysis Version 7.0 for Bigger Datasets. *Mol. Biol. Evol.* **33**, 1870-1874 (2016).
24. J. D. Thompson, D. G. Higgins, T. J. Gibson, CLUSTAL W: improving the sensitivity of progressive multiple sequence alignment through sequence weighting, position-specific gap penalties and weight matrix choice. *Nucleic Acids Res.* **22**, 4673-4680 (1994).
25. P. Caffrey, Conserved amino acid residues correlating with ketoreductase stereospecificity in modular polyketide synthases. *ChemBioChem* **4**, 654-657 (2003).
26. J. H. Sulston, J., The nematode *Caenorhabditis elegans*. *Cold Spring Harbor Laboratory* **17**, 988 (1988).
27. S. Bleuler-Martínez *et al.*, A lectin-mediated resistance of higher fungi against predators and parasites. *Mol. Ecol.* **20**, 3056-3070 (2011).
28. M. P. Smith *et al.*, A liquid-based method for the assessment of bacterial pathogenicity using the nematode *Caenorhabditis elegans*. *FEMS Microbiol. Lett.* **210**, 181-185 (2002).
29. J. Schindelin *et al.*, Fiji: an open-source platform for biological-image analysis. *Nat. Methods* **9**, 676-682 (2012).
30. C. T. Rueden *et al.*, ImageJ2: ImageJ for the next generation of scientific image data. *BMC Bioinform.* **18**, 529 (2017).
31. Z. Cseresnyes, K. Kraibooj, M. T. Figge, Hessian-based quantitative image analysis of host-pathogen confrontation assays. *Cytometry A* **93**, 346-356 (2018).
32. D. Legland, I. Arganda-Carreras, P. Andrey, MorphoLibJ: integrated library and plugins for mathematical morphology with Image J. *Bioinformatics* **32**, 3532-3534 (2016).